Published in final edited form as:
*Biochim Biophys Acta*. 2012 March ; 1821(3): 502–512. doi:10.1016/j.bbalip.2011.08.019.

# Dysfunctional HDL Containing L159R ApoA-I Leads to Exacerbation of Atherosclerosis in Hyperlipidemic Mice

**Mary G. Sorci-Thomas**[a,*], **Manal Zabalawi**[a,1], **Manish S. Bharadwaj**[a,1], **Ashley J. Wilhelm**[a], **John S. Owen**[b], **Bela F. Asztalos**[c], **Shaila Bhat**[a], and **Michael J. Thomas**[b]

[a]Department of Pathology, Section on Lipid Sciences, Jean Mayer U.S. Department of Agriculture Human Nutrition Research Center on Aging at Tufts University, Boston, MA, USA

[b]Center for Lipid Science, and Biochemistry, Jean Mayer U.S. Department of Agriculture Human Nutrition Research Center on Aging at Tufts University, Boston, MA, USA

[c]Wake Forest School of Medicine, Winston-Salem; and Lipid Metabolism Laboratory, Jean Mayer U.S. Department of Agriculture Human Nutrition Research Center on Aging at Tufts University, Boston, MA, USA

## Abstract

The mutation L159R apoA-I or apoA-$I_{L159R}$ (FIN) is a single amino acid substitution within the sixth helical repeat of apoA-I. It is associated with a dominant negative phenotype, displaying hypoalphaproteinemia and an increased risk for atherosclerosis in humans. Mice lacking both mouse apoA-I and LDL receptor (LDL$^{-/-}$, apoA-I$^{-/-}$) (double knockout or DKO) were crossed > 9 generations with mice transgenic for human FIN to obtain L159R apoA-I, LDLr$^{-/-}$, ApoA-I$^{-/-}$ (FIN-DKO) mice. A similar cross was also performed with human wild-type (WT) apoA-I (WT-DKO). In addition, FIN-DKO and WT-DKO were crossed to obtain WT/FIN-DKO mice. To determine the effects of the apoA-I mutations on atherosclerosis, groups of each genotype were fed either chow or an atherogenic diet for 12 weeks. Interestingly, the production of dysfunctional HDL-like particles occurred in DKO and FIN-DKO mice. These particles were distinct with respect to size, and their enrichment in apoE and cholesterol esters. Two-dimensional gel electrophoresis indicated that particles found in the plasma of FIN-DKO mice migrated as large $\alpha_3$-HDL. Atherosclerosis analysis showed that FIN-DKO mice developed the greatest extent of aortic cholesterol accumulation compared to all other genotypes, including DKO mice which lack any apoA-I. Taken together these data suggest that the presence of large apoE enriched HDL particles containing apoA-I L159R lack the normal cholesterol efflux promoting properties of HDL, rendering them dysfunctional and pro-atherogenic. In conclusion, large HDL-like particles containing apoE and apoA-$I_{L159R}$ contribute rather than protect against atherosclerosis, possibly through defective efflux properties and their potential for aggregation at their site of interaction in the aorta.



[*]Address correspondence to: Mary G. Sorci-Thomas, Department of Pathology, Section on Lipid Sciences, Wake Forest School of Medicine, Medical Center Blvd, Winston-Salem, NC 27157, Tel.: +1 336 716 2417; Fax: +1 336 716 6279. msthomas@wakehealth.edu.
[1]Both authors contributed equally to this work.

**Keywords**

Apolipoprotein A-1; Apolipoprotein A-$1_{FIN}$; Atherosclerosis; Dysfunctional HDL; L159R ApoA-I

## 1. Introduction

Numerous human epidemiological studies have demonstrated an inverse correlation between plasma HDL concentrations and the risk for coronary heart disease in humans [1]. Studies in animal models have complimented these findings [2, 3], since transgenic and knockout mouse studies have shown that circulating HDL apoA-I primarily plays a protective function and slows the progression of atherosclerosis through the process called reverse cholesterol transport (RCT) [4]. In the process of RCT apoA-I accepts free cholesterol from peripheral tissues by interacting with ATP binding cassette transporter A1 (ABCA1) to form nascent HDL (nHDL) [5, 6]. The free cholesterol in nHDL is then esterified by lecithin cholesterol acyltransferase (LCAT) and the nHDL particles mature to form cholesterol ester-enriched spherical particles where apoA-I acts as a cofactor for LCAT [7]. Numerous studies have demonstrated that a specific domain of apoA-I, consisting of the sixth and seventh α-helical repeats (amino acid residues 143–186 of the mature protein), was essential for the activation of LCAT [8, 9]. A second major role for apoA-I in protecting against cardiovascular disease is through the modulation of inflammation [10–13].

From a total of approximately 50 naturally occurring human mutations which result in secretion of full-length apoA-I, less than half are associated with lower than average plasma concentrations of HDL apoA-I with about nineteen of these mutations shown to reduce the capacity of apoA-I to activate LCAT. Mutations associated with abnormal LCAT activation are centered within repeats 5, 6, and 7 corresponding to amino-acids 121 to 186. A subset of these nineteen are located within a domain between residues 143–186, or helices 6 and 7 displaying a dominant negative effect on plasma HDL apoA-I concentrations [14]. It has been estimated that structural mutations within apoA-I occur in around 0.3% of the Japanese population which may directly affect the plasma concentrations HDL [15] as well as its function.

There have been reports describing mutations that lead to low concentrations of HDL apoA-I for which little or no association to CHD has been demonstrated in affected individuals. One well known apoA-I variant, apoA-$I_{Milano}$ or apoA-$I_{R173C}$ [16], has been associated with a degree of cardioprotection despite low concentrations of plasma HDL. The former is characterized by having ineffective LCAT-cofactor activity but normal lipid binding and cholesterol efflux-promoting abilities [17–21]. First identified in the northwestern tip of Italy this mutation represents an amino acid substitution of cysteine for arginine at position 173 (R173C) in the seventh helical repeat of apoA-I. The resulting apoA-$I_{Milano}$/apoA-$I_{Milano}$ homodimers have enhanced RCT. Affected subjects with HDL deficiency show reduced CHD event rates and reduced carotid intima media thickness [22]. However, in hypercholesterolemic mice replacement of wild-type mouse apoA-I with human apoA-$I_{R173C}$ did not show any protective advantage, rather female mice expressing human apoA-$I_{R173C}$ showed higher lipid deposition in their aortas [23]. On the other hand, these studies showed that hepatic secretion of the mutant protein was severely compromised and played a major role in determining the low levels of circulating HDL [24].

Another well studied single amino acid substitution within the sixth helical repeat, L159R apoA-I (apoA-$I_{L159R}$), or apoA-$I_{FIN}$, (FIN) was identified in a kindred from Finland [25]. Affected family members were hypo-α lipoproteinemic, heterozygous for the mutation and had only 20% as much plasma HDL cholesterol and 25% as much plasma apoA-I as

unaffected family members. ApoA-$I_{L159R}$ thus belongs to a group of apoA-I mutations described as displaying a dominant negative phenotype. Studies showed no impaired cholesterol efflux from fibroblasts to phospholipid complexed apoA-$I_{L159R}$ [25], but HDL containing apoA-$I_{L159R}$ did show accelerated clearance from plasma presumably due to the inability of the mutant apoA-I to activate LCAT [26]. This and other studies have shown that delayed HDL particle maturation associated with apoA-$I_{L159R}$ [27, 28] can explain a portion of the mechanism for the observed dominant negative phenotype in individuals carrying a single allele for this mutation. In other studies, apoA-$I_{L159R}$ was overexpressed in mice using adenovirus and in this study the authors concluded that proteolytic degradation could explain the dominant negative phenotype and its effect on apoA-$I_{WT}$ concentrations in heterozygotes [29]. In addition, these authors investigated apoA-I secretion using cultured primary mouse hepatocytes following treatment with adenoviral vectors expressing the mutant protein and mixtures of wild-type and mutant apoA-I. They found severely impaired secretion of apoA-$I_{L159R}$ from hepatocytes that was attributable to intracellular misfolding, aggregation and subsequent proteolysis.

The present study was undertaken to investigate the role of apoA-$I_{L159R}$ containing HDL in the development of atherosclerosis. To do this hypercholesterolemic mice carrying apoA-$I_{L159R}$ were created and fed an atherogenic diet for 12 weeks. Previous studies from our lab [30, 31] and others [32, 33] have shown that low density lipoprotein receptor (LDLr) and apoA-I double knockout (DKO) mice ($LDL^{-/-}$, apoA-$I^{-/-}$) are useful hypercholesterolemic models for studying atherosclerosis [34]. In this manuscript, we report the consequences of expressing apoA-$I_{L159R}$ in DKO mice, were associated with the formation of dysfunctional HDL and an increase in the development of atherosclerosis. Our data show that apoA-$I_{L159R}$ expression was associated with the increased conversion of large apoE rich particles to proatherogenic particles that promote the development of atherosclerosis.

## 2. Materials and Methods

### 2.1. Materials

Sterile 100μm nylon mesh, 60 mm collagen coated plates, 24-Gauge and 0.75 in. catheters were from BD Medical Systems Inc. (Franklin Lakes, NJ). Collagenase was from Worthington Biochemical (Lakewood, NJ). William's Medium E, nitrocellulose membrane, Trizol Reagent and protein G-sepharose beads were from Invitrogen (Carlsbad, CA). Bovine serum albumin, Coomassie brilliant blue G, Triton X-100, PMSF, leupeptin, pepstatin, glucose, hygromycin, penicillin, streptomycin, glutamine and Corning EIA/RIA 96 well plates were from Sigma-Aldrich (St. Louis, MO). DMEM was from Mediatech, Inc. (Manassas, VA). Fetal bovine serum was from Atlanta Biologicals (Lawrenceville, GA). KBr was from Fisher Scientific (Pittsburgh, PA). Kits for analysis of total plasma cholesterol and triglycerides were from Roche Molecular Biomedical (Indianapolis, IN). Amicon Ultra concentrators and Amicon Ultra-15 Filter Devices were from Millipore (Billerica, MA). Goat anti-human apolipoprotein A-1 antibody was purchased from Millipore (Temecula, CA). The Phospholipids C analysis kit was from Wako Diagnostics (Richmond, VA). The OmniScript RT kit was from Quaigen (Valencia, CA). Random primers were from Promega (Fitchburg, WI). Microisolater TM cages were from Lab products (Maywood, NJ). High molecular weight standards, elutip-D minicolumns, Superdex-200 10/3000GL columns and Superose 6 columns were from GE Healthcare (Piscataway, NJ). All other reagents were of the highest grade commercially available.

### 2.2. Animals and Diet

The production of transgenic mice expressing human apoA-$I_{L159R}$ (FIN) was prepared by polymerase chain reaction primer mutagenesis using a 0.7-kilobase *Kpn*I/*Hpa*I DNA

fragment of the human apoA-I gene. This 0.7-kilobase fragment was ligated into the *Kpn*I/*Hpa*I site of the 4.92-kilobase pLIVLE6 a liver specific construct kindly obtained from John M. Taylor [35]. The whole construct was digested with *Spe*I/*Not*I and then ligated on the corresponding *Spe*I/*Not*I site in the 3-kilobase vector pBSSK. This construct was used to transform *E.coli* ER2566 cells for obtaining more copies of the construct. After the transformed DNA was isolated from the *E.coli* ER2566 cells the construct was then digested with *Spe*I/*Not*I and the 6-kilobase pLIVLE6 construct was purified using elutip-D minicolumns. The production of transgenic mice was out by DNA microinjection into C57BL/6J × DBA embryos (B6D2F1 embryos) using standard techniques. Following weaning of founder mice, a mouse tail biopsy of approximately 1 cm in length was used for DNA analysis by polymerase chain reaction for the presence of the mutant apoA-I transgene. All mice were maintained in specific pathogen-free barrier facilities in Microisolater TM caging and were fully crossed into the LDLr receptor and apoA-I double knockout ($LDLr^{-/-}$, $apoA\text{-}I^{-/-}$ or DKO) background for > 9 generations to obtain FIN-DKO mice [30, 34, 36]. Transgenic human $apoA\text{-}I_{WT}$ mice were obtained from Charles River Laboratories (Bar Harbor, ME) and were also crossed into the DKO background to obtain WT-DKO mice. Crosses between FIN-DKO and WT-DKO were also carried out to obtain WT FIN -DKO mice. From our analysis the DNA copy numbers were approximately 100 for FIN-DKO, 200 for WT FIN-DKO and 200 for WT-DKO.

All mice were housed at the Wake Forest University Medical Center. The Animal Care and Use Committee of the Wake Forest University School of Medicine approved all procedures. Experimental mice were weaned at 30 days and fed Purina chow. At 6 weeks of age, a group of mice from each genotype were fed an atherogenic diet containing 10% saturated fat from palm oil and 0.1% cholesterol for approximately 12 weeks [30, 31, 37]. As controls both gender and age matched mice from each genotype were fed chow for 12 weeks. All mice were maintained in a temperature-controlled room with 12-hour light and 12-hour dark cycle.

### 2.3. Tissue RT-PCR

RNA was isolated from fresh tissue using Trizol Reagent according to the manufacturer's instructions. The concentration of purified RNA was determined from the OD at 260 nm. 1 μg of total RNA was used for cDNA synthesis employing reverse transcription with random primers from Promega and an OmniScript RT kit. Real-time quantitative PCR was performed using an Applied Biosystems 7000 (Carlsbad, CA) sequence detector following the manufacturer's suggestions. For negative controls reverse transcriptase was omitted at the time of cDNA synthesis to determine the extent of genomic DNA contamination. Primers were created using Primer Express software (Applied Biosystems, Carlsbad, CA) and synthesized by IDT (Coralville, Iowa, IA). All values are relative to mouse GAPDH and normalized to an age-matched WT-DKO mouse for the appropriate genotype and tissue using the ΔΔCt method as previously described [30]. All human apoA-I primer sequences are available upon request.

### 2.4. Plasma Lipoprotein Analysis, Isolation and Characterization

Plasma was collected from anesthetized fasting mice by cardiac puncture. Blood was centrifuged at 10,000 rpm for 10 min (4°C). Plasma was removed and stored at −80°C as described previously [30]. Plasma from both chow- and diet-fed mice was analyzed for total plasma cholesterol and triglycerides by enzymatic assay. To isolate the total lipoprotein fraction, plasma was subjected to density-gradient ultracentrifugation. Approximately 1 mL of chow- fed and 500 μL of diet-fed plasma were adjusted to 1.225 g/mL with KBr and centrifuged at 50,000 rpm for 18 h (4°C). The top 3 mL from each centrifuge tube was dialyzed against 10 mM ammonium bicarbonate, pH=7.4.

To separate into lipoprotein classes, the d<1.225 fraction was applied to 2 Superose-6 columns connected in tandem and eluted at 0.5 mL/min with 0.9% NaCl, 2.6 μM EDTA and 1.5 μM sodium azide. Total cholesterol was determined in each fraction by enzymatic assay. Classes of lipoproteins for chow and diet plasma were pooled using the cholesterol distribution profile. Chow plasma classes of lipoproteins were pooled into VLDL/LDL fractions #40–65, LDL/HDL transition particles fractions #66–73 and HDL fractions #74–85. Diet plasma classes of lipoproteins were pooled into VLDL/LDL fractions #40–60, LDL/HDL transition particles fractions #61–69 and HDL fractions #70–85. After pooling all fractions were concentrated using Amicon Ultra concentrators before being assayed for lipid composition. Triglycerides, free, and esterified cholesterol were assayed using kits from Roche Molecular Biochemical. Phospholipids were assayed using a kit from Wako Diagnostics. Total protein was determined by the method of Lowry [38]. To assess the VLDL/LDL, LDL/HDL and HDL fractions apolipoprotein composition, an equivalent of 10 μg protein of chow and diet pooled fractions were run on 12% SDS-PAGE as previously described [36].

### 2.5. Plasma Apolipoprotein Quantification

Plasma concentrations of human apoA-$I_{WT}$ and apoA-$I_{L159R}$ were determined using a combination of Enzyme-Linked Immunosorbent Assay (ELISA) and mass spectrometry [39], as previously described. Plasma mouse apoE was determined by ELISA, in which a 96 well plate was coated with WUE4 purified anti-apoE that was kindly provided by Dr. Holtzman. Purified apo-E protein and $apoE^{-/-}$ plasma were used as standards and negative control, respectively. Both were kindly provided by Dr. Weisgraber. Samples were diluted in ELISA sample buffer and then treated as previously described [40]. Plates were read at 650 nm and mouse apoE concentration in plasma was expressed as mg/dL.

### 2.6. Measurement of the L159R - Wild-Type ApoA-I Ratio

Standards for the ratio determination of L159R to wild-type apoA-I were prepared from pure stocks of the two proteins as previously described [39]. Serial dilutions were used to generate five standards, each containing 1 μg of total protein. These standard proteins preparations were loaded onto individual lanes of a 12% SDS-PAGE and analyzed by trypsin digestion and liquid chromatography-mass spectrometry (LC-MS) [41] in parallel with mouse plasma samples.

Peptide mixtures from each trypsin digestion were analyzed by LC-MS on a Waters Q-TOF API-US mass spectrometer running MassLynx™ 4.0 software, connected to a Waters CapLC through an Advion Nanomate source. The HPLC column was a 100 μm × 100 mm Waters Symmetry $C_{18}$ column with 3.5 μm particle size. Samples were injected in water containing 0.02% formic acid at 0.5 μl/min. The column was eluted with Solvent A for 12 min, followed by a linear gradient to 80% Solvent B over 8 min, then holding at 80% B for 10 min before returning to the initial conditions. Solvent A was water:acetonitrile (99:1) with 0.2% formic acid, and Solvent B was water:acetonitrile (3:97) with 0.2% formic acid. Positive ion electrospray spectra from *m/z* 300–1600 were recorded in continuum mode with a 2.4 second accumulation time. Chromatographic peak areas for the $[M+2H]^{2+}$ charge states of the wild-type and L159R versions of the T25 peptide were plotted against the ratio of protein amounts to generate a calibration curve [39].

### 2.7. Isolation of Mouse Primary Hepatocytes

Hepatocytes were isolated using a previously described method [42]. Briefly, mice were anesthetized and the inferior vena cava was cannulated using a 24 gauge, 0.75 in. catheter. The liver was then pre-perfused at 5 mL/min with a $Ca^{2+}$ deficient solution for 10 min followed by 0.3mg/mL collagenase solution containing 5 mM $CaCl_2$ for 10–18 min. The

liver was removed and hepatocytes were isolated from the liver by mechanical dissociation in William's Medium E containing 10% fetal bovine serum and filtered through a sterile 100μm nylon mesh. Cells were plated at a density of $6 \times 10^5$ cells/60 mm collagen coated plates containing 10% FBS in William's Medium. Cells were allowed to attach for 2 h at after which the medium was replaced and the cells were incubated overnight. Cell culture was carried out in a humidified chamber at 37°C, 5% $CO_2$.

### 2.8. Pulse-Chase Labeling and ApoA-I Immunoprecipitation

The pulse was carried out as previously described [36] except that 200 μCi of $^{35}$S Met/Cys was added to each 60 mm plate containing $6 \times 10^5$ cells for 45 min. The chase was initiated by aspirating the labeling medium and then adding 1 mL of methionine-free DMEM-FBS. At the indicated intervals the medium was separated from cell pellets and both were adjusted to final concentration of 1 mg/ml BSA and then immunoprecipitated by adding 5 μL of goat anti-human apoA-I antibody and 40 μL of Protein G-Sepharose beads. After incubating overnight at 4°C on a rotating wheel, immune complexes were recovered by centrifugation at 12,000 rpm for 5 min. ApoA-I was eluted from the Protein G-Sepharose beads then separated by 12% SDS-PAGE as previously described [36, 43]. Gels containing $^{35}$S-labeled apoA-I were dried and the radioactivity associated with each band determined using a FUJIFILM BAS-5000 Imaging Plate Scanner (Stamford, CT).

### 2.9. Production and Characterization of Nascent HDL

**2.9.1. Cell Culture—**Human embryonic kidney (HEK) 293 cells expressing ABCA1 were a generous gift from Dr. Michael Hayden, University of British Columbia, Canada and supplied by Dr. John Parks [44, 45]. Cells were maintained in Dulbeccos' minimum essential medium (DMEM) containing 4.5 g/L glucose, 50 μg/mL hygromycin, 100 U/mL penicillin, 100 μg/mL streptomycin, 2 mM L-glutamine and 10% FBS. Cells were maintained at 37°C in an atmosphere of 5% $CO_2$. ABCA1 expressing cells were plated in 100 mm dishes until cells reached ~90% confluence. To remove traces of contaminating serum proteins, cells were washed 4 times with phosphate buffered saline, then 10 mL of serum-free DMEM was added and the cells were incubated for 1 h at 37°C. This media was then removed and another 10 mL of serum-free DMEM was added for second 1 h incubation. Following this incubation 10 mL of fresh DMEM containing 10 μg/mL of $^{125}$I-labeled lipid-free human apoA-$I_{WT}$ [46 ], apoA-$I_{R173C}$ (Milano) [47] or apoA-$I_{L159R}$ (FIN) [36, 39] was added and incubated overnight at 37°C as previously described [44]. The next day the culture media was harvested and dialyzed against 10 mM ammonium bicarbonate, pH 7.4 at 4°C then concentrated using Amicon Ultra-15 Filter Devices. In parallel experiments HEK 293 Flp-In™ cells (Invitrogen, Carlsbad, CA), which do not express ABCA1 were treated with lipid-free apoA-I in the same manner.

**2.9.2. Isolation and Purification of nHDL—**Concentrated culture media was fractionated by fast protein liquid chromatography (FPLC) using 3 Superdex-200 10/3000GL (GE Healthcare) columns connected in series at a flow rate of 0.3 ml/min. Each fraction was counted to determine its radioactive content and then plotted vs fraction number. For mass analysis, all fractions corresponding to nHDL were pooled and an aliquot assayed for apoA-I content using ELISA, as previously described [48]. In addition, aliquots from each of the 4 peak fractions were also analyzed by 4–30% non-denaturing gradient gel electrophoresis (NDGGE) to determine the particle diameter size homogeneity and compared to high molecular weight standards. Radioactive protein bands were visualized on the gel using a BAS 5000 phosphorimager (Fujifilm).

**2.9.3. Lipid Extraction of nHDL—**Lipids were extracted from the dried nHDL peaks #1–4, according to Bligh and Dyer [49], adding 4 μg of [3,4-$^{13}C_2$]cholesterol as the internal

standard for cholesterol analyses. Lipid extracts were evaporated under a stream of argon, dissolved in 1 mL of chloroform : methanol (1:1) and stored at −80°C until analyzed. In all cases, parallel experiments were conducted using non-ABCA1 expressing cells and those results subtracted from the values obtained from ABCA1-expressing cells.

**2.9.4. Cholesterol Analysis—**An aliquot was evaporated under argon, dissolved in toluene and then analyzed on a Thermo Scientific TSQ Quantum XLS mass spectrometer interfaced to a Trace gas chromatograph. One μL of the reconstituted sample was injected in the splitless mode onto a 30 m × 250 μm DB-1 column (J&W Scientific) having a 0.25 μm film thickness. Helium carrier gas was set at 2 ml/min. The temperature program was as follows: 150 °C for 1 min, 150°C to 280 °C at 25 °C/min, ending at 280 °C for 23 min. The samples were ionized by positive-ion electron impact with selected ion monitoring (SIM) of *m/z* 386.4 for cholesterol and *m/z* 388.4 for [3,4-$^{13}C_2$]cholesterol. A second 50 μL aliquot was saponified at room temperature for 2 h with ethanolic-KOH, similar to a reported procedure [50] cooled and then extracted with hexane. After evaporation under argon the residue was dissolved in 20 μL of toluene and analyzed for cholesterol content. Cholesterol ester was calculated from the difference between the total cholesterol and free cholesterol values. All analyses were performed in glass vessels. A standard curve was prepared for quantitation.

**2.9.5. Phospholipid Analysis—**Phospholipid in nHDL samples was quantified using the lipid phosphorus analysis [51].

## 2.10. Lipoprotein Size Analysis

To assess plasma lipoprotein particle size after FPLC 10 μg of protein from pooled fractions were run on 4–30% nondenaturing gradient gel electrophoresis (NDGGE) as described previously. Gels were stained with Comassie brilliant blue G, destained and their image recorded using an Alpha Innotech Imaging system (Cell Biosciences, Santa Clara, CA) as previously described [30]. Particle size was determined by comparison with high molecular weight standards of known Stoke's diameter.

To characterize HDL subpopulations two-dimensional gel electrophoresis was performed, as described previously [52]. In the first dimension, HDL particles were separated on agarose according to charge (pre-β, α and pre-α) based on their relative mobility to albumin. In the second dimension HDL particles were separated by size on a nondenaturing PAGE followed by electrotransfer to a nitrocellulose membrane. Membranes were probed with anti-apoA-1 antibody to localize each apoA-I containing particle using anti-human albumin antibody to mark the α-front.

## 2.11. Atherosclerosis Assessment

To assess the development of atherosclerosis in each of the mouse genotypes after 12 weeks on the atherogenic diet, male and female mice began diet at 6 weeks of age. After 12 wk of diet they were anesthetized then opened through the midline exposing the thoracic and abdominal cavity. The heart and aorta were perfused with saline to remove blood then removed and suspended in 10% formalin for at least 48 h before further analysis. Atherosclerosis evaluations were carried out as previously described [30]. Briefly, the heart and aorta were placed under dissecting microscope and the adventitia completely removed. Lipids were extracted from the entire aorta using the method of Folch [53]. Both Free and total cholesterol content was determined by gas-liquid chromatography. After extraction the protein residue was digested in 1 N NaOH and the total protein content per aorta measured by the Lowry method [38]. Aortic cholesterol was expressed as μg of cholesterol per mg protein.

### 2.12. Statistical Analysis

Values are presented as the mean ± SD. All groups were compared for all possible combinations using a student's t test, with $p<0.05$ considered as statistically significant.

## 3. Results

### 3.1. Genotypes employed

To study the effect of the apoA-$I_{L159R}$ mutation on cholesterol metabolism and atherosclerosis we created transgenic mice expressing the human L159R apoA-I mutation. These mice were crossed for > 9 generations into mice lacking both mouse apoA-I and LDL receptor, designated double knockout or DKO mice, called FIN-DKO mice [39]. Mice transgenic for human apoA-$I_{WT}$ were also crossed into the DKO background to generate apoA-$I_{WT}$, apoA-$I^{-/-}$, $LDLr^{-/-}$ mice, or WT-DKO mice. WT-DKO mice were crossed with FIN-DKO mice to obtain transgenic mice that expressed both apoA-$I_{WT}$ and apoA-$I_{L159R}$, called WT FIN-DKO mice. DNA copy number ranged between 100–200 copies per liver cell in all genotypes used, while, the mRNA abundance were 1.5-fold and 5-fold respectively for WT-DKO, and WT FIN-DKO compared to FIN-DKO which was set at 1.0, as determined by RT-PCR (data not shown).

### 3.2. Plasma lipoprotein cholesterol

All genotypes of mice (between 9–60 males and female mice) were age and gender matched and fed either an atherogenic diet containing 10% saturated fat from palm oil and 0.1% cholesterol or chow for 12 weeks. Table 1 shows important plasma lipoprotein and apolipoprotein parameters for all four genotypes of mice fed chow or the atherogenic diet. The total plasma cholesterol (TPC) concentration for DKO, WT-DKO, FIN-DKO, and WT FIN-DKO were similar when fed chow. On the atherogenic diet FIN-DKO mice had a statistically significant lower TPC (750 ± 32 mg/dL) compared to WT-DKO mice (1201 ± 68 mg/dL). WT FIN-DKO mice had TPC levels (850 ± 46 mg/dL) about equal to the FIN-DKO, but much less than that of WT-DKO.

In response to the atherogenic diet the WT-DKO mice had the largest increase in VLDL/LDL particles, as shown by the FPLC separation illustrated in Fig. 1. To measure these changes FPLC profiles were obtained from the plasma of chow- and diet-fed mice from each of the various genotypes. **Panel A of** Fig. 1 shows the FPLC profiles for mice fed chow while **Panel B**, Fig. 1, shows profiles for atherogenic diet-fed mice. WT-DKO and WT FIN-DKO had well defined peaks corresponding to HDL sized particles. In contrast, FIN-DKO and DKO plasma had very little HDL sized particles consistent with the absence of wild-type apoA-I in their plasma. WT FIN-DKO plasma had an HDL peak comparable to that in WT-DKO thus indicating that WT FIN-DKO restores the HDL levels in apoA-$I_{L159R}$ expressing mice. The atherogenic diet increased the VLDL/LDL fraction with WT-DKO showing the largest change, while FIN-DKO had the smallest change.

### 3.3. Plasma apolipoprotein concentrations

Since human apoA-$I_{L159R}$ carriers have low plasma HDL levels compared to normal human counterparts [25], we measured plasma apoA-I and apoE levels and the results are summarized in Table 1. To complement these measurements SDS-PAGE analysis, shown in Fig. 2, was performed on plasma samples. The concentrations of protein migrating at ~28 kDa, corresponding to apoA-I, and protein migrating at ~38 kDa, corresponding to apoE, changed in response to both genotype and diet. As expected apoA-$I_{L159R}$ levels in FIN-DKO mice were 10–20-fold lower compared to apoA-$I_{WT}$ in WT-DKO mice, 5.0 ± 1.0 mg/dL versus 100.0 ± 6.0 mg/dL, respectively (Table 1 and Fig 2). This large difference in

plasma levels did not appear to be due to either transgenic DNA copy number or mRNA abundance, as determined by RT-PCR (data not shown).

ApoA-$I_{WT}$ and apoA-$I_{L159R}$ have almost identical molecular masses and are equally reactive with our polyclonal antibodies. Therefore, to assess plasma apoA-$I_{L159R}$ levels where apoA-$I_{WT}$ was co-expressed, e.g. the plasma of WT FIN-DKO mice, we quantified the tryptic peptides that included the mutated or unmutated site at 159 (T25) as we have previously reported [39]. Surprisingly, the plasma concentration of apoA-$I_{WT}$ in WT FIN-DKO, 113 ± 10 mg/dL, was not significantly lower than that measured in plasma from WT-DKO mice. Total plasma apoA-I in WT FIN-DKO, was slightly greater than the plasma level of WT-DKO for either chow, 138 mg/dL ( WT + FIN apoA-I) versus 100 mg/dL, or diet fed mice, 167 mg/dL (WT + FIN apoA-I) versus 126 mg/dL, respectively. This was the opposite of what we had expected because the apoA-$I_{L159R}$ has been reported to have a dominant negative effect on apoA-$I_{WT}$ levels in humans. The WT FIN-DKO mouse model was created to mimic the heterozygous state of apoA-$I_{WT}$ and apoA-$I_{L159R}$ in humans, but this mouse model differed in its plasma apoA-I levels compared to its human counterpart.

However, the expression of apoA-$_{WT}$ increased the plasma concentration apoA-$I_{L159R}$ 5-fold in WT FIN-DKO mice (Table 1) suggesting that the secretion of apoA-$I_{WT}$ facilitated the secretion of apoA-$I_{L159R}$. On an atherogenic diet the level of plasma apoA-$I_{L159R}$ and apoA-$I_{WT}$ increased only slightly over chow levels. Plasma levels of mouse apoE were influenced by the presence of FIN-mutation as well as diet as seen in Table 1 and Fig. 2. On a chow diet plasma apoE levels increased about 2-fold in apoA-$I_{L159R}$ expressing mice compared to plasma from DKO and WT-DKO mice. Atherogenic diet fed DKO and FIN-DKO mice showed about a 2- to 3-fold increase in plasma apoE over chow fed controls, while mice expressing apoA-$I_{WT}$ had a 4- to 5-fold increase in plasma apoE concentrations over chow fed mice.

### 3.4. Production and Secretion of apoA-$I_{WT}$ and apoA-$I_{L159R}$

Given the low levels of apoA-$I_{L159R}$ protein in FIN DKO mouse plasma, we conducted pulse-chase experiments on primary mouse hepatocytes using $^{35}$S-Met. Studies were conducted in three genotypes, FIN-DKO, WT-DKO and FIN WT-DKO in order to determine the effect of apoA-$I_{L159R}$ expression on the secretion of apoA-$I_{WT}$. Fig. 3 Panel A shows newly synthesized apoA-I immunoprecipitated from the cell pellet while Panel B shows the apoA-I immunoprecipitated from the medium of pulsed-chased primary mouse hepatocytes. FIN-DKO hepatocytes produced only low levels of apolipoprotein when compared to WT-DKO mice. Interestingly, hepatocytes from WT FIN-DKO livers synthesized and secreted apoA-I at a rate about a quarter of that measured for WT-DKO hepatocytes, which was not expected considering the plasma concentration (Table 1). However, in other studies exploring the synthesis and secretion of apoA-$I_{L159R}$ from adenoviral treated mouse hepatocytes [29] a very similar finding was reported. These data suggest that apoA-$I_{L159R}$ not only was produced at low levels, but that it interfered with the secretion of apoA-$I_{WT}$ making it susceptible to intracellular degradation. Therefore, low levels of plasma apoA-$I_{L159R}$ are likely due to misfolding of the mutant protein during synthesis and its entry into the quality control pathway. Besides the demonstration of this using hepatocytes, similar observations have been reported for apoA-$I_{L159R}$ transfected COS cells and other helix 6 mutations [36]. Although pulse chase experiments showed apoA-$I_{L159R}$ expression reduced the amount apoA-$I_{WT}$ leaving the hepatocytes, plasma HDL levels were unchanged in WT FIN-DKO mice (Table 1). In fact, the level of apoA-$I_{L159R}$ in the plasma of WT FIN-DKO mice actually increased (Table 1) suggesting a significant contribution of intravascular metabolism once the lipidated particles gain entry into the plasma compartment.

We also examined the lipidation of apoA-$I_{L159R}$ and apoA-$I_{WT}$ by ABCA1 expressing cells, as seen in Fig. 3 Panels C and D. In Fig. 3 Panel C shows the lipidation of lipid-free $^{125}$I-apoA-$I_{WT}$ (circles) and $^{125}$I-apoA-$I_{L159R}$ (diamonds) and demonstrated that there was an approximately 4–5-fold reduction in the amount of radioactive nascent HDL containing apoA-$I_{L159R}$ compared to apoA-$I_{WT}$ containing HDL (note difference in left and right Y axis). When the mass of nascent HDL particles produced from ABCA1 expressing cells was measured, as shown in Fig. 3 panel D, the mass of glycerophosphatidylcholine (GP), cholesterol and apoA-I confirmed the inability of apoA-$I_{L159R}$ to efficiently form nascent HDL particles. These data are consistent with previous studies showing the misfolding of a number of other helix 6 apoA-I mutations, leading to formation of cytosolic phospholipid inclusions and eventual degradation by cellular quality control pathways [36].

### 3.5. L159R apoA-I mutation contributes to formation of dysfunctional HDL

To assess the size and composition of particles formed in response to the L159R mutation three fractions from the FPLC separation of mouse plasma (Fig. 1) were analyzed by nondenaturing gradient gel electrophoresis as shown in Fig. 4 and by SDS PAGE as shown in Fig. 5. Fraction I (**FX1**) contained mostly apoB and apoE and, therefore, was designated the VLDL/LDL fraction. Fraction II (**FX2**) contained some apoB, greater amounts of apoE and some apoA-I and was designated as transition particles (LDL/HDL). Finally, fraction III (**FX3**) contained mainly apoE (~36kD) and apoA-I (~28kD) and was designated HDL.

On chow both FIN-DKO and DKO mice have more apoE in FX1 and FX2 as compared to WT-DKO and WT FIN-DKO, which have distinct HDL sized particles which correspond to FX3 (Fig. 4). When challenged with an atherogenic diet all genotypes show increased content of apoE (Fig. 4 and Table 1), but again DKO and FIN-DKO have higher apoE than WT-DKO and WT FIN-DKO.

In FX2, the LDL/HDL transition particles, the size of the particles change dramatically in response to diet, as shown in Fig. 5 **Panel A**. Again, the DKO and FIN DKO shows greater amounts of large particles above the 17 nm marker, which only increase with diet (Fig. 5 **Panel B**). The apolipoprotein content shown in Fig. 4 of FX2 shows a greater content of apoE in these particles that tended to increase with diet. In comparison, WT-DKO and WT FIN DKO have very little of the large apoE enriched particles in FX2 (Fig. 4) and have instead a transition particle with a diameter of 9.8 nm, as shown in Fig. 5, that contained apoA-I, but very little apoE (Fig. 4).

For FX3 the HDL fraction was essentially the same between chow and diet-fed mice for all genotypes. Interestingly, again DKO and FIN-DKO mice were more similar to each other than to the WT-DKO and WT FIN-DKO with respect to particle size (Fig. 5) and apolipoprotein content (Fig. 4). WT-DKO and FIN WT-DKO mouse plasma contained ~3 different sized HDL particles running at about 7.5, 8.2 and 10.8 nm, while the DKO mice had a broad smear with 2 bands at 10.0 and 13.8 nm, and FIN-DKO mouse plasma did not show well-defined particles (Fig. 5). However, from the SDS PAGE of FX3 shown in Fig. 4 it is clear that there was significant apoE and mutant apoA-I present in these particles, which contribute to the concept that these are “dysfunctional” HDL particles.

To further investigate the HDL subpopulations in the various genotypes additional studies were performed using two-dimensional (2-D) gel electrophoresis. Fig. 6 shows the 2-D HDL subpopulation analysis for three genotypes of mice fed an atherogenic diet. Fig. 6 **Panel A** shows that WT-DKO mouse plasma contains pre-β, α1, α2 and α3 as well as pre-α1, pre-α2, and pre-α3 particles. Fig. 6 **Panel B** shows FIN-DKO plasma on the other hand had very few α particles and did not show any pre-β or pre-α particles. In contrast, Fig. 6 **Panel C** shows the profile for WT FIN-DKO plasma demonstrating that adding apoA-$I_{W}$T to FIN-

DKO gives a plasma profile similar to WT-DKO. These results agreed well with the FPLC profiles (Fig. 1) of these genotypes, suggesting that the low levels of HDL in FIN-DKO plasma was due to the total loss of pre-β and pre-α particles. The small amount of HDL present in plasma was in the form of α particles.

### 3.6. Free and Esterified Cholesterol Ratio

The free to ester cholesterol composition for each of the 3 fractions corresponding to VLDL/LDL, LDL/HDL and HDL or FX1, FX2, and FX3 for all genotypes are shown in Fig. 7 as stacked bars where the total cholesterol is divided into free and esterified cholesterol. Fig. 7 **Panel A** shows the results for chow fed mice, while Fig. 7 **Panel B** shows the content for atherogenic diet fed mice. For chow-fed mice DKO and FIN-DKO had similar TC contents while WT-DKO and WT FIN-DKO were again very similar to each other. For both DKO and FIN-DKO most of the cholesterol was contained in FX1 (VLDL/LDL), whereas, mice expressing apoA-$I_W$T had a more equitable distribution of cholesterol between FX1 (VLDL/LDL) and FX3 (HDL). The EC/TC ratio was similar among all genotypes and fractions (EC/TC = 0.6–0.7) except for FX3 of both DKO (0.5) and FIN-DKO (0.3).

In contrast, for diet-fed mice as shown in Fig. 7 **Panel B** WT-DKO was shown to have the greatest increase in cholesterol content and this occurred mainly in FX1. Interestingly, both DKO and FIN-DKO had the greatest cholesterol content in FX2 or the LDL/HDL fraction and as expected little cholesterol in FX3. The EC/TC ratio was similar among all genotypes and fractions (EC/TC = 0.6–0.7) except for FX3 of FIN-DKO (0.5). Other lipids were analyzed among all genotypes and showed that total triglycerides were not significantly different between genotypes (data not shown).

### 3.7. Atherosclerosis evaluation

Age and gender matched mice from each of the four genotypes were fed an atherogenic diet for 12 wk after which the aortas were analyzed for their total cholesterol content. Fig. 8 shows the cholesterol content of aortas from each genotype expressed as μg cholesterol/mg protein. Interestingly, the greatest level of cholesterol accumulation was found in the FIN-DKO mice followed by DKO mice. The least amount of cholesterol accumulation in the aorta was found in the mice that expressed apoA-$I_{WT}$. These results suggest that having small amount of apoA-$I_{L159R}$-containing HDL was more atherogenic than not expressing any apoA-I and, therefore, having no HDL.

## 4. Discussion

In humans a single apoA-I amino acid substitution within helix 6 of apoA-I corresponding to L159R was found associated with hypo-α lipoproteinemia having only 20% of HDL concentrations when compared to unaffected family members [25]. All affected individuals were heterozygous suggesting that apoA-$I_{L159R}$ belonged to a group of apoA-I mutations displaying a dominant negative phenotype on wild-type apoA-I levels in plasma. Humans that express the L159R–mutation did not show clinical signs of coronary artery disease, but because of the reduced levels of HDL were considered to be at increased risk for developing the disease [25]. However, our results demonstrated that expression of apoA-$I_{L159R}$ in hypercholesterolemic mice leads to a significantly greater level of atherosclerosis than in the absence of apoA-$I_{WT}$. Interestingly, despite the lower plasma cholesterol levels in both FIN-DKO and DKO mice, these genotypes had higher aortic cholesterol deposition than WT-DKO or WT-FIN-DKO mice. Therefore, these data suggest that particles containing apoA-$I_{L159R}$, were dysfunctional and pro-atherogenic (Fig. 8) and likely not competent in their ability to accept and mobilize cholesterol. The reason for the contribution of apoA-$I_{L159R}$ particles to the development of atherosclerosis may be related to the unstable conformation

of the apoA-$I_{L159R}$ protein [36], combined with its association with an increase concentration of large apoE rich transition particles which appear to contribute to the greater aortic cholesterol deposition. Interestingly, although the low levels of apoA-$I_{L159R}$ produced by hepatocytes and then lipidated by ABCA1 appear to have a dominant effect on the folding and lipidation of apoA-$I_{WT}$ (Fig.3) in the hepatocytes, once the HDL particles enter the plasma this effect is gone. Therefore, these data suggest that plasma levels of HDL apoA-I are regulated to a greater extent by intravascular metabolism, and particle remodeling and explain the loss of the dominant negative effect at the plasma level (Table 1).

In other attempts to model dominant negative mutants, apoA-$I_{R173C}$, was studied using either transgenic mice [17, 18] or knockin mice [23, 24] in these studies the presence of the mutant apoA-I protein also did not have the “dominant negative” feature that has been observed in humans. Specifically, using knockin mice for apoA-I Milano or R173C apoA-I, there was no difference in the plasma apoA-I concentration between mice carrying two alleles of the mutant protein and mice carrying one mutant and one wild-type allele [24]. Similar to our results the apoA-IMilano knockin mice did show impaired secretion of mutant protein and an intermediate level of secretion when the mutant and wild-type protein were secreted together. This suggests that a dominant effect on the secretion of the wild-type allele does occur but is not evident by simple examination of the plasma protein levels alone.

In addition, our pulse chase experiments in transgenic mouse hepatocytes also agree with the results from adenovirus mediated expression of L159R apoA-I [29], since secretion of apoA-$I_{L159R}$ was greatly reduced compared to apoA-$I_{WT}$. Also similar were results when hepatocytes expressed both apoA-$I_{L159R}$ and apoA-$I_{WT}$ [29]. In fact, in the adenovirus infected apoA-I knockout mice, the plasma apoA-I concentration were not different between apoA-$I_{L159R}$ only expressing mice and mice expressing both apoA-$I_{WT}$ and apoA-$I_{L159R}$ mice [29]. Therefore, using various modes of expressing dominant negative mutant forms of apoA-I in mice, there exists a disconnect between the effects of mutation at the secretion level and the plasma concentration. It could be speculated that this disconnect is related to the degree of hypercholesterolemia in LDL receptor knockout mice or to the fact that mice lack CETP. However, neither of these possibilities are likely since the apoA-I Milano knockin mice had functioning LDL receptors [23, 24], and studies in L159R apoA-I mice expressing the human CETP transgene similar trends to those data presented here were observed (M. Zabalawi, M. Bharadwaj, unpublished data).

The plasma profiles of different genotypes fed either chow or diet showed that mice expressing apoA-$I_{WT}$ had high concentrations of HDL apoA-I (Fig. 1) while mice carrying apoA-$I_{L159R}$ had significantly reduced plasma apoA-I. These findings are consistent with a number of other studies in mice expressing L159R apoA-I [27, 29]. Another important finding was that apoE levels were greater in both genotypes that had low levels of plasma apoA-I, DKO and FIN-DKO. Plasma from DKO mice had little to no HDL-sized particles while FIN-DKO mice had a small amount of material that ran in the HDL-sized region and which, like the DKO mice, contained considerable amounts of apoE, but little apoA-I (Table 1). Nondenaturing gradient gel electrophoresis analyses showed that the expression of apoA-$I_{WT}$ yielded plasma HDL particles of well defined sizes (Fig. 5). However, in the absence of apoA-I DKO mice had only low levels of HDL-sized particles. Instead, they had increased amounts of particles referred to as LDL/HDL transitional particles, which contain apoB and apoE. Likewise, expression of apoA-$I_{L159R}$ did not generate well-defined plasma HDL particles, but showed a significant increase in the amount of particles that run in the LDL size range (Figs. 1 and 5) and carried both apoB an apoE (Fig. 4). Two-dimensional analysis of mouse plasma showed that FIN-DKO mouse plasma contained significantly reduced

amounts of all HDL fractions, preβ, preα and α-HDL, compared to WT-DKO and WT FIN-DKO (Fig. 6). These results suggest that in the absence of apoA-I cholesterol mobilization calls for increased participation of apoE.

In all instances the amounts of free and esterified cholesterol carried by each class were similar for DKO and FIN-DKO (Fig. 7). For both, the cholesterol profiles were similar on each diet. On an atherogenic diet there was a considerable increase in the mass of cholesterol carried by LDL/HDL or transition particles and HDL fractions compared to the VLDL/LDL fraction. This increase in mass was associated with an increase in particle size or diameter (Fig. 5). On chow WT-DKO mouse plasma had slightly more cholesterol in the VLDL/LDL fraction than did WT FIN-DKO mice, which had more in the HDL fraction. On a fat-enriched diet the distinction was even greater with a dramatic increase in the VLDL/LDL fraction in plasma from WT-DKO mice. Surprisingly, WT-DKO plasma from mice fed the fat-rich diet showed a substantial increase in cholesterol carried by VLDL/LDL, the fraction rich in apoB and apoE, compared to the other genotypes.

## 5. Conclusions

We conclude that in primary mouse hepatocytes the co-expression of the FIN mutation with WT reduces apoA-I secretion to 25% compared to WT by itself. Because mRNA levels for apoA-I are not reduced the affect of the FIN mutation is most likely on the secretion and lipidation steps. In mice the co-expression of apoA-$I_{WT}$ along with apoA-$I_{L159R}$ gave plasma concentrations similar to WT alone. This situation is very different from that of humans heterozygous for FIN and WT apoA-I where plasma apoA-I levels are about 25% of normal patients. However, no mouse model to date has been capable of modeling the dominant negative phenotype as seen in humans. What is curious about the mouse is that even with reduced secretion of apoA-I in mice expressing both wild-type and L159R apoA-I, the plasma concentration was similar, with an actual increase in the concentration of the apoA-$I_{L159R}$, suggesting rescue of the protein on apoA-$I_{WT}$ containing particles. These results suggest that, although the synthesis of apoA-$I_{wt}$ is inhibited the synthesis and secretion are sufficiently rapid compared to catabolism so that apoA-I could achieve a normal steady-state concentration.

Most importantly these studies show that the expression of low levels of the apoA-$I_{L159R}$ mutation significantly increased the extent of atherosclerosis, even greater than mice having no plasma apoA-I at all. The mechanism responsible for this appears to be the increase formation of LDL/HDL transition particles containing L159R apoA-I that appear to be dysfunctional in their ability to remove cholesterol and may in fact exacerbate delivery of cholesterol to the artery wall.

## Acknowledgments

We thank Dr. Holtzman of the Washington University School of Medicine, Department of Neurology, Molecular Biology and Pharmacology for providing us with the WUE4 apoE antibody. We also thank Dr. Weisgraber of the Gladstone Institute of Cardiovascular and Neurological Disease, University of California for providing us with purified mouse apoE. These studies were supported by grants from the National Heart, Lung, and Blood Institute, National Institutes of Health (HL-49373 and HL-64163 to MGS-T). The Q-TOF was purchased with funds from NIH Shared Instrumentation Grant 1 S10 RR17846 (MJT) and the Advion Nanomate Source was from the North Carolina Biotechnology Center grant 2007-IDG-1021 (MJT). MS analyses were performed in the Mass Spectrometer Facility of CCCWFU School of Medicine and supported in part by NCI center grant 5P30CA12197.

## Abbreviations

| | |
|---|---|
| **(apoA-I)** | apolipoprotein A-I |

| | |
|---|---|
| **(apoA-$I_{WT}$)** | unmutated apolipoprotein A-I |
| **(ABCA1)** | ATP binding cassette transporter A1 |
| **(CHD)** | coronary heart disease |
| **(ELISA)** | enzyme-linked immunosorbent assay |
| **(FPLC)** | fast protein liquid chromatography |
| **(apoA-$I_{L159R}$)** | FIN-mutation of apolipoprotein A-I |
| **(FX1)** | Fraction 1 |
| **(FX2)** | Fraction 1 |
| **(FX3)** | Fraction 3 |
| **(HEK)** | human embryonic kidney cells |
| **(LCAT)** | lecithin cholesterol acyltransferase |
| **(LC-MS)** | liquid chromatography-mass spectrometry |
| **(LDLr)** | low density lipoprotein receptor |
| **(nHDL)** | nascent HDL |
| **(rHDL)** | recombinant HDL |
| **(RCT)** | reverse cholesterol transport |
| **(SIM)** | selected ion monitoring |
| **(SDS-PAGE)** | sodium dodecyl sulfate-polyacrylamide gel electrophoresis |
| **(DKO)apoA-$I_{L159R}$** | low density lipoprotein receptor and apoA-I double knockout mice |

## References


1. Gordon T, Castelli WP, Hjortland MC, Kannel WB, Dawber TR. High density lipoprotein as a protective factor against coronary heart disease. The Framingham Study. Am J Med. 1977; 62:707–714. [PubMed: 193398]
2. Voyiaziakis E, Goldberg IJ, Plump AS, Rubin EM, Breslow JL, Huang LS. ApoA-I deficiency causes both hypertriglyceridemia and increased atherosclerosis in human apoB transgenic mice. J Lipid Res. 1998; 39:313–321. [PubMed: 9507992]
3. Rubin EM, Krauss RM, Spangler EA, Verstuyft JG, Clift SM. Inhibition of early atherogenesis in transgenic mice by human apolipoprotein A-I. Nature. 1991; 353:265–267. [PubMed: 1910153]
4. Rader DJ. High-density lipoproteins and atherosclerosis. Am J Cardiol. 2002; 90:62i–70i.
5. Lawn RM, Wade DP, Garvin MR, Wang X, Schwartz K, Porter JG, Seilhamer JJ, Vaughan AM, Oram JF. The Tangier disease gene product ABC1 controls the cellular apolipoprotein-mediated lipid removal pathway. J Clin Invest. 1999; 104:R25–R31. [PubMed: 10525055]
6. Vaughan AM, Oram JF. ABCA1 redistributes membrane cholesterol independent of apolipoprotein interactions. J Lipid Res. 2003; 44:1373–1380. [PubMed: 12700343]
7. Rothblat GH, Phillips MC. High-density lipoprotein heterogeneity and function in reverse cholesterol transport. Curr Opin Lipidol. 2010; 21:229–238. [PubMed: 20480549]
8. Sorci-Thomas MG, Thomas M, Curtiss L, Landrum M. Single repeat deletion in apoA-I blocks cholesterol esterification and results in rapid catabolism of D6 and wild-type apoA-I in transgenic mice. J Biol Chem. 2000; 275:12156–12163. [PubMed: 10766851]
9. Sorci-Thomas M, Kearns MW, Lee JP. Apolipoprotein A-I domains involved in lecithin-cholesterol acyltransferase activation. Structure:function relationships. J Biol Chem. 1993; 268:21403–21409. [PubMed: 8407982]

10. Tall AR, Yvan-Charvet L, Terasaka N, Pagler T, Wang N. HDL, ABC transporters and cholesterol efflux: implications for the treatment of atherosclerosis. Cell Metab. 2008; 7:365–375. [PubMed: 18460328]
11. Yvan-Charvet L, Wang N, Tall AR. Role of HDL, ABCA1, and ABCG1 transporters in cholesterol efflux and immune responses. Arterioscler Thromb Vasc Biol. 2010; 30:139–143. [PubMed: 19797709]
12. Oram JF, Vaughan AM. ATP-Binding cassette cholesterol transporters and cardiovascular disease. Circ Res. 2006; 99:1031–1043. [PubMed: 17095732]
13. Tang C, Liu Y, Kessler PS, Vaughan AM, Oram JF. The macrophage cholesterol exporter ABCA1 functions as an anti-inflammatory receptor. J Biol Chem. 2009; 284:32336–32343. [PubMed: 19783654]
14. Sorci-Thomas MG, Thomas MJ. The effects of altered apolipoprotein A-I structure on plasma HDL concentration. Trends Cardiovasc Med. 2002; 12:121–128. [PubMed: 12007737]
15. Yamakawa-Kobayashi K, Yanagi H, Fukayama H, Hirano C, Shimakura Y, Yamamoto N, Arinami T, Tsuchiya S, Hamaguchi H. Frequent occurrence of hypoalphalipoproteinemia due to mutant apolipoprotein A-I gene in the population: a population-based survey. Hum Mol Genet. 1999; 8:331–336. [PubMed: 9931341]
16. Weisgraber KH, Bersot TP, Mahley RW, Franceschini G, Sirtori CR. A-$I_{Milano}$ Apoprotein. Isolation and characterization of a cysteine-containing variant of the A-I apoprotein from human high density lipoproteins. J Clin Invest. 1980; 66:901–907. [PubMed: 6776144]
17. Chiesa G, Stoltzfus LJ, Michelagnoli S, Bielicki JK, Santi M, Forte TM, Sirtori CR, Franceschini G, Rubin EM. Elevated triglycerides and low HDL cholesterol in transgenic mice expressing human apolipoprotein A-I(Milano). Atherosclerosis. 1998; 136:139–146. [PubMed: 9544740]
18. Bielicki JK, Forte TM, McCall MR, Stoltzfus LJ, Chiesa G, Sirtori CR, Franceschini G, Rubin EM. High density lipoprotein particle size restriction in apolipoprotein A-I(Milano) transgenic mice. J Lipid Res. 1997; 38:2314–2321. [PubMed: 9392429]
19. Bielicki JK, McCall MR, Stoltzfus LJ, Ravandi A, Kuksis A, Rubin EM, Forte TM. Evidence that apolipoprotein A-IMilano has reduced capacity, compared with wild-type apolipoprotein A-I, to recruit membrane cholesterol. Arterioscler Thromb Vasc Biol. 1997; 17:1637–1643. [PubMed: 9327756]
20. Alexander ET, Weibel GL, Joshi MR, Vedhachalam C, de la Llera-Moya M, Rothblat GH, Phillips MC, Rader DJ. Macrophage reverse cholesterol transport in mice expressing ApoA-I Milano. Arterioscler Thromb Vasc Biol. 2009; 29:1496–1501. [PubMed: 19661486]
21. Weibel GL, Alexander ET, Joshi MR, Rader DJ, Lund-Katz S, Phillips MC, Rothblat GH. Wild-type ApoA-I and the Milano variant have similar abilities to stimulate cellular lipid mobilization and efflux. Arterioscler Thromb Vasc Biol. 2007; 27:2022–2029. [PubMed: 17615385]
22. Sirtori CR, Calabresi L, Franceschini G, Baldassarre D, Amato M, Johansson J, Salvetti M, Monteduro C, Zulli R, Muiesan ML, Agabiti-Rosei E. Cardiovascular status of carriers of the apolipoprotein A-I(Milano) mutant: the Limone sul Garda study. Circulation. 2001; 103:1949–1954. [PubMed: 11306522]
23. Parolini C, Chiesa G, Gong E, Caligari S, Cortese MM, Koga T, Forte TM, Rubin EM. Apolipoprotein A-I and the molecular variant apoA-I(Milano): evaluation of the antiatherogenic effects in knock-in mouse model. Atherosclerosis. 2005; 183:222–229. [PubMed: 16285990]
24. Parolini C, Chiesa G, Zhu Y, Forte T, Caligari S, Gianazza E, Sacco MG, Sirtori CR, Rubin EM. Targeted replacement of mouse apolipoprotein A-I with human ApoA-I or the mutant ApoA-IMilano. Evidence of APOA-IM impaired hepatic secretion. J Biol Chem. 2003; 278:4740–4746. [PubMed: 12471038]
25. Miettinen HE, Gylling H, Miettinen TA, Viikari J, Paulin L, Kontula K. Apolipoprotein A-IFin. Dominantly inherited hypoalphalipoproteinemia due to a single base substitution in the apolipoprotein A-I gene. Arterioscler Thromb Vasc Biol. 1997; 17:83–90. [PubMed: 9012641]
26. Miettinen HE, Jauhiainen M, Gylling H, Ehnholm S, Palomaki A, Miettinen TA, Kontula K. Apolipoprotein A-IFIN (Leu159-->Arg) mutation affects lecithin cholesterol acyltransferase activation and subclass distribution of HDL but not cholesterol efflux from fibroblasts. Arterioscler Thromb Vasc Biol. 1997; 17:3021–3032. [PubMed: 9409289]

27. Koukos G, Chroni A, Duka A, Kardassis D, Zannis VI. LCAT can rescue the abnormal phenotype produced by the natural ApoA-I mutations (Leu141Arg)Pisa and (Leu159Arg)FIN. Biochemistry. 2007; 46:10713–10721. [PubMed: 17711302]
28. Zannis VI, Koukos G, Drosatos K, Vezeridis A, Zanni EE, Kypreos KE, Chroni A. Discrete roles of apoA-I and apoE in the biogenesis of HDL species: lessons learned from gene transfer studies in different mouse models. Ann Med. 2008; 40(Suppl 1):14–28. [PubMed: 18246469]
29. McManus DC, Scott BR, Franklin V, Sparks DL, Marcel YL. Proteolytic degradation and impaired secretion of an apolipoprotein A-I mutant associated with dominantly inherited hypoalphalipoproteinemia. J Biol Chem. 2001; 276:21292–21302. [PubMed: 11292828]
30. Zabalawi M, Bhat S, Loughlin T, Thomas MJ, Alexander E, Cline M, Bullock B, Willingham M, Sorci-Thomas MG. Induction of fatal inflammation in LDL receptor and ApoA-I double-knockout mice fed dietary fat and cholesterol. Am J Pathol. 2003; 163:1201–1213. [PubMed: 12937162]
31. Zabalawi M, Bharadwaj M, Horton H, Cline M, Willingham M, Thomas MJ, Sorci-Thomas MG. Inflammation and skin cholesterol in LDLr−/−, apoA-I−/− mice: link between cholesterol homeostasis and self-tolerance? J Lipid Res. 2007; 48:52–65. [PubMed: 17071966]
32. Moore RE, Navab M, Millar JS, Zimetti F, Hama S, Rothblat GH, Rader DJ. Increased Atherosclerosis in Mice Lacking Apolipoprotein A-I Attributable to Both Impaired Reverse Cholesterol Transport and Increased Inflammation. Circ Res. 2005; 97:763–771. [PubMed: 16151025]
33. Moore RE, Kawashiri MA, Kitajima K, Secreto A, Millar JS, Pratico D, Rader DJ. Apolipoprotein A-I Deficiency Results in Markedly Increased Atherosclerosis in Mice Lacking the LDL Receptor. Arterioscler. Thromb. Vasc. Biol. 2003; 23:1914–1920. [PubMed: 12933536]
34. Wilhelm AJ, Zabalawi M, Grayson JM, Weant AE, Major AS, Owen J, Bharadwaj M, Walzem R, Chan L, Oka K, Thomas MJ, Sorci-Thomas MG. Apolipoprotein A-I and its role in lymphocyte cholesterol homeostasis and autoimmunity. Arterioscler Thromb Vasc Biol. 2009; 29:843–849. [PubMed: 19286630]
35. Simonet WS, Bucay N, Lauer SJ, Taylor JM. A far-downstream hepatocyte- specific control region directs expression of the linked human apolipoprotein E and C-I genes in transgenic mice. J Biol Chem. 1993; 268:8221–8229. [PubMed: 7681840]
36. Bhat S, Zabalawi M, Willingham MC, Shelness GS, Thomas MJ, Sorci- Thomas MG. Quality control in the apoA-I secretory pathway: deletion of apoA-I helix 6 leads to the formation of cytosolic phospholipid inclusions. J Lipid Res. 2004; 45:1207–1220. [PubMed: 15060083]
37. Rudel LL, Kelley K, Sawyer JK, Shah R, Wilson MD. Dietary monounsaturated fatty acids promote aortic atherosclerosis in LDL receptor-null, human apoB100 -overexpression transgenic mice. Arterioscler Thromb Vasc Biol. 1998; 18:1818–1827. [PubMed: 9812923]
38. Lowry OH, Rosebrough NJ, Farr AL, Randall RJ. Protein measurement with the Folin phenol reagent. J Biol Chem. 1951; 19:265–275. [PubMed: 14907713]
39. Owen JS, Bharadwaj MS, Thomas MJ, Bhat S, Samuel MP, Sorci-Thomas MG. Ratio determination of plasma wild-type and L159R apoA-I using mass spectrometry: tools for studying apoA-IFin. J Lipid Res. 2007; 48:226–234. [PubMed: 17071967]
40. Sorci-Thomas M, Hendricks CL, Kearns MW. HepG2 cell LDL receptor activity and the accumulation of apolipoprotein B and E in response to docosahexaenoic acid and cholesterol. J Lipid Res. 1992; 33:1147–1156. [PubMed: 1431595]
41. Bhat S, Sorci-Thomas MG, Alexander ET, Samuel MP, Thomas MJ. Intermolecular contact between globular N-terminal fold and C-terminal domain of ApoA-I stabilizes its lipid-bound conformation: studies employing chemical cross-linking and mass spectrometry. J Biol Chem. 2005; 280:33015–33025. [PubMed: 15972827]
42. Nelson LJ, Newsome PN, Howie AF, Hadoke PW, Dabos KJ, Walker SW, Hayes PC, Plevris JN. An improved ex vivo method of primary porcine hepatocyte isolation for use in bioartificial liver systems. Eur J Gastroenterol Hepatol. 2000; 12:923–930. [PubMed: 10958220]
43. Shelness GS, Morris-Rogers KC, Ingram MF. Apolipoprotein B48-Membrane Interactions. Absence of transmembrane localization to nonhepatic cells. J Biol Chem. 1994; 269:9310–9318. [PubMed: 8132669]

44. Mulya A, Lee JY, Gebre AK, Thomas MJ, Colvin PL, Parks JS. Minimal lipidation of pre-beta HDL by ABCA1 results in reduced ability to interact with ABCA1. Arterioscler Thromb Vasc Biol. 2007; 27:1828–1836. [PubMed: 17510466]
45. See RH, Caday-Malcolm RA, Singaraja RR, Zhou S, Silverston A, Huber MT, Moran J, James ER, Janoo R, Savill JM, Rigot V, Zhang LH, Wang M, Chimini G, Wellington CL, Tafuri SR, Hayden MR. Protein kinase A site-specific phosphorylation regulates ATP-binding cassette A1 (ABCA1)-mediated phospholipid efflux. J Biol Chem. 2002; 277:41835–41842. [PubMed: 12196520]
46. Wilhelm AJ, Zabalawi M, Owen JS, Shah D, Grayson JM, Major AS, Bhat S, Gibbs DP Jr. Thomas MJ, Sorci-Thomas MG. Apolipoprotein A-I modulates regulatory T cells in autoimmune LDLr−/− ApoA-I−/− mice. J Biol Chem. 2010; 285:36158–36169. [PubMed: 20833724]
47. Bhat S, Sorci-Thomas MG, Calabresi L, Samuel MP, Thomas MJ. Conformation of dimeric apolipoprotein A-I milano on recombinant lipoprotein particles. Biochemistry. 2010; 49:5213–5224. [PubMed: 20524691]
48. Sorci-Thomas MG, Parks JS, Kearns MW, Pate GN, Zhang C, Thomas MJ. High level secretion of wild-type and mutant forms of human proapoA-I using baculovirus-mediated Sf-9 cell expression. J Lipid Res. 1996; 37:673–683. [PubMed: 8728328]
49. Bligh EG, Dyer WJ. A rapid method of total lipid extraction and purification. Can J Biochem Physiol. 1959; 37:911–917. [PubMed: 13671378]
50. Nordskog BK, Reagan JW Jr. St Clair RW. Sterol synthesis is up-regulated in cholesterol-loaded pigeon macrophages during induction of cholesterol efflux. J Lipid Res. 1999; 40:1806–1817. [PubMed: 10508200]
51. Rouser G, Siakotos AN, Fleischer S. Quantitative analysis of phospholipids by thin-layer chromatography and phosphorus analysis of spots. Lipids. 1966; 1:85–86. [PubMed: 17805690]
52. Asztalos BF, Schaefer EJ. High-density lipoprotein subpopulations in pathologic conditions. Am J Cardiol. 2003; 91:12E–17E. [PubMed: 12505564]
53. Folch J, Lees M, Sloane Stanley GH. A simple method for the isolation and purification of total lipides from animal tissues. J Biol Chem. 1957; 226:497–509. [PubMed: 13428781]

## Highlights

- Atherosclerosis was studied in mice expressing only mutant apoA-$I_{L159R}$ (FIN-DKO).
- Most apoA-$I_{L159R}$ synthesized in mouse hepatocytes was retained and degraded.
- ApoA-$I_{L159R}$ reduced the secretion of apoA-$I_{WT}$ when expressed together.
- ApoA-$I_{L159R}$ had no effect on plasma levels of HDL or apoA-$I_{WT}$.
- HDL-like particles from FIN-DKO mice contained large amounts of apoE and B.
- FIN-DKO mice had increased aortic cholesterol compared to mice lacking apoA-I.

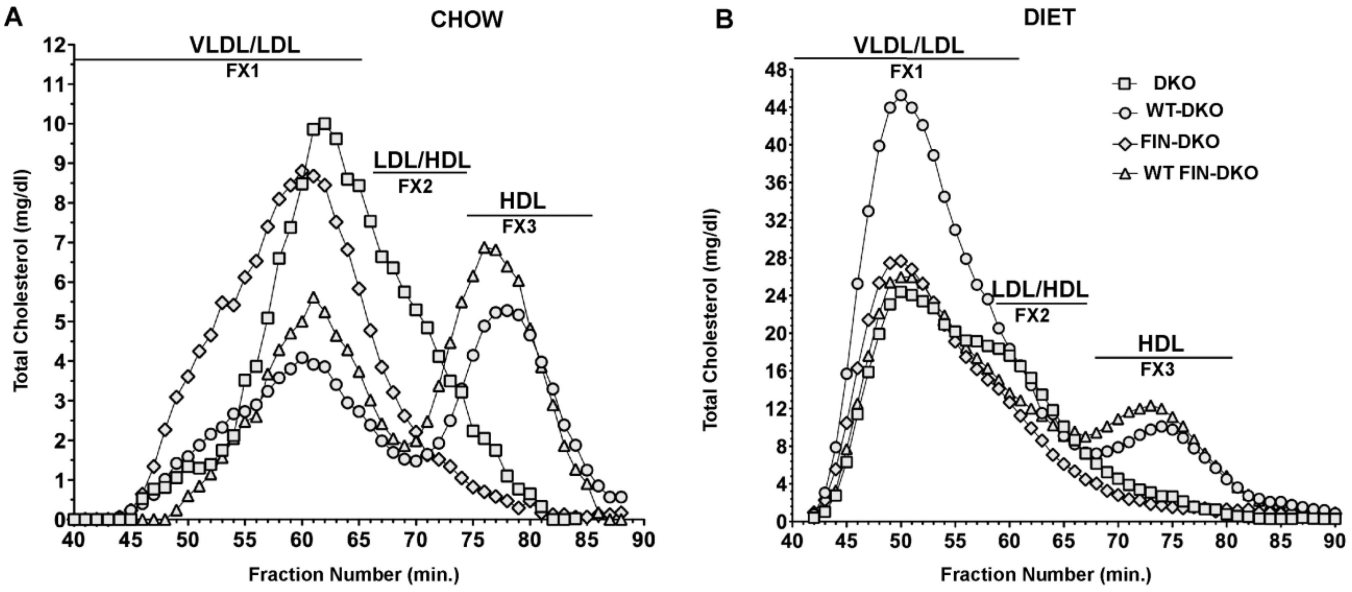


Figure 1

**Figure 1. Lipoprotein Cholesterol Distribution After FPLC of Mouse Plasma**

Panel A shows the cholesterol distribution for chow-fed and Panel B shows the distribution for atherogenic diet-fed mouse plasma. After approximately 12 wks of chow or diet, whole mouse plasma was ultracentrifuged to obtain the d<1.225 total lipoprotein fraction, which was then separated into various lipoprotein classes by FPLC. Then the total cholesterol concentration in each fraction was measured by enzymatic assay and expressed as mg/dL of plasma. All techniques used here are described in “Materials and Methods”. Mouse genotype abbreviations are: LDLr$^{-/-}$, apoA-I$^{-/-}$ = DKO; Transgenic human apoA-I$_{WT}$, LDLr$^{-/-}$, apoA-I$^{-/-}$ = WT-DKO; transgenic human apoA-I$_{L159R}$, LDLr$^{-/-}$, apoAI$^{-/-}$ = FIN-DKO; transgenic apoA-I$_{WT}$ and apoA-I$_{L159R}$, LDLr$^{-/-}$, apoA-I$^{-/-}$ = WT FIN-DKO. The profile for each genotype was obtained from an individual mouse’s plasma, however numerous profiles for each genotype were run to ensure reproducibility.

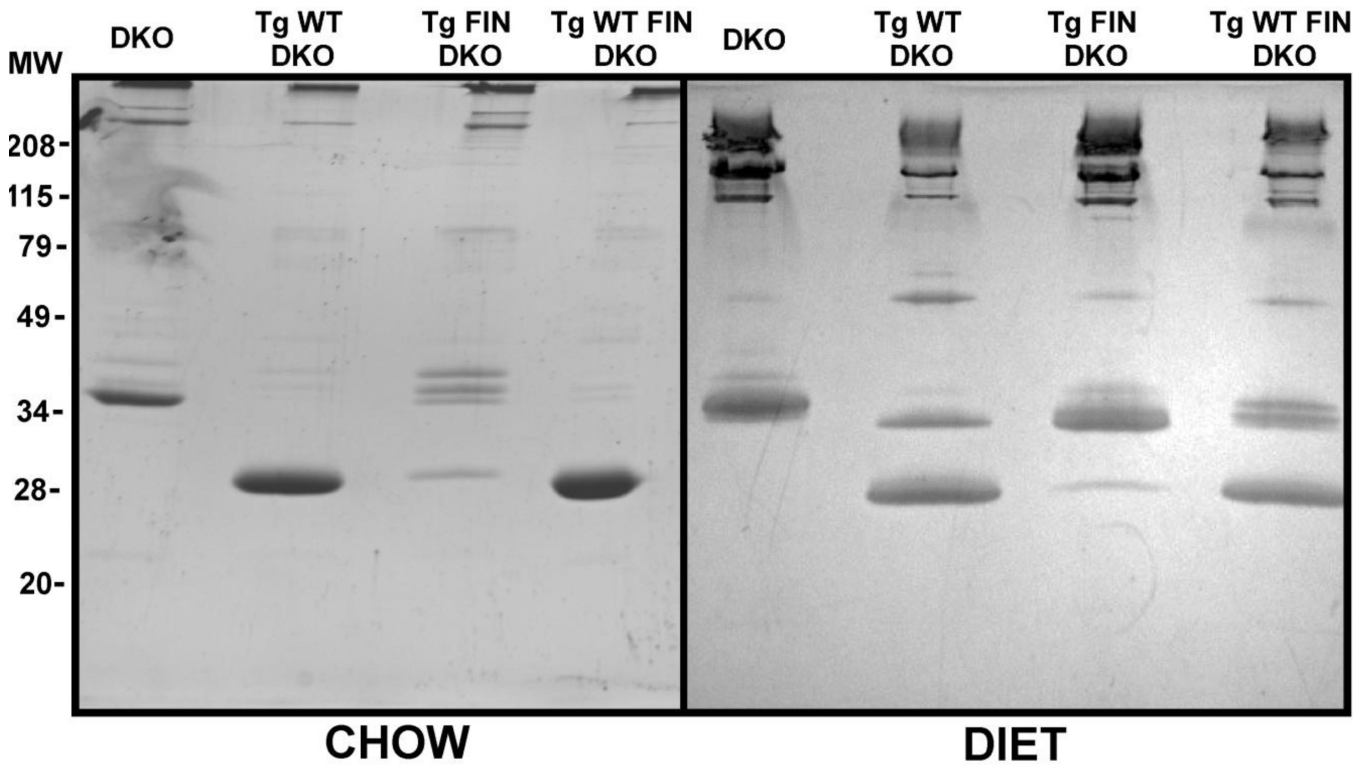


**Figure 2. SDS-PAGE of Chow- and Diet-fed Mouse Plasma**

Panel A shows apoprotein distribution from chow-fed and Panel B atherogenic diet-fed mouse plasma top (d<1.225). After approximately 12 wks of chow or diet whole mouse plasma was centrifuged to obtain the d<1.225 total lipoprotein fraction as described in "Materials and Methods." The total protein was determined by method of Lowry [38] and an equivalent of 10 μg of protein per lane were run and stained as described in "Materials and Methods." Mouse genotype abbreviations are the same as in Figure 1.

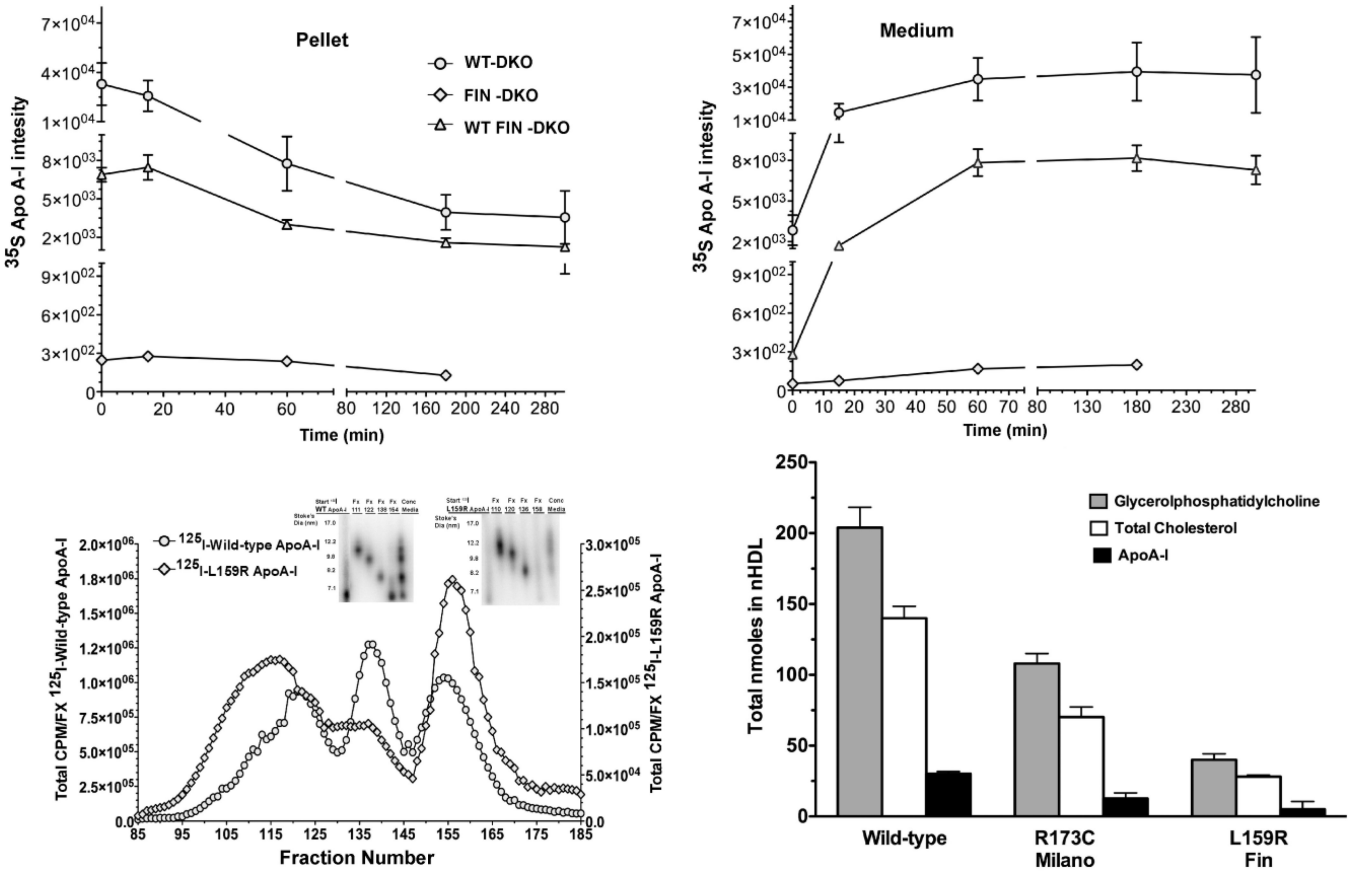


**Figure 3. Expression of Wild-type and L159R ApoA-I**

Panel A and B shows the expression of newly synthesized apoA-I from primary mouse hepatocytes that were pulsed-chased with $^{35}$S-Met, immunoprecipitation and run on SDS PAGE. Newly synthesized apoA-I disappearance from the cell pellet Panel A, (circles) hepatocytes from WT-DKO mice ;(diamond) hepatocytes from FIN-DKO mice and (triangle) from WT FIN-DKO mice and appears in the culture medium Panel B. Data was obtained from imaging and plotted as $^{35}$S intensity, as described in " Materials and Methods." Panel C shows the size distribution of lipidated apoA-I (or nascent HDL) particles after incubation with ABCA1 expressing HEK cells incubated with 10 μg/ml of lipid-free human $^{125}$I-apoA-I in serum free media for 18 hrs. Following the incubation the medium was removed, concentrated and separated using FPLC. The radioactive content of each fraction was determined and plotted as the percent of total $^{125}$I-apoA-I$_{WT}$ (circles) and apoA-I$_{L159R}$ (diamonds) per fraction. Inset shows 4–30% nondenaturing gradient gel electrophoresis. Radioactive protein bands were visualized on the gel using phosphorimaging; Panel D, shows the total nmole of the two major classes of lipids. Compositional analysis indicated that the major lipids comprising nHDL particles were glycerophospholipid (GP) shown in shaded bars, and cholesterol shown in open bars. Total cholesterol was measured using GC/MS methodology while GP was analyzed using LC/MS/MS and cholesterol by GC/MS as described in "Materials and Methods.". All values represent the mean ± S.D of 3 to 4 independent experiments. Mouse genotype abbreviations are the same as in Figure 1.

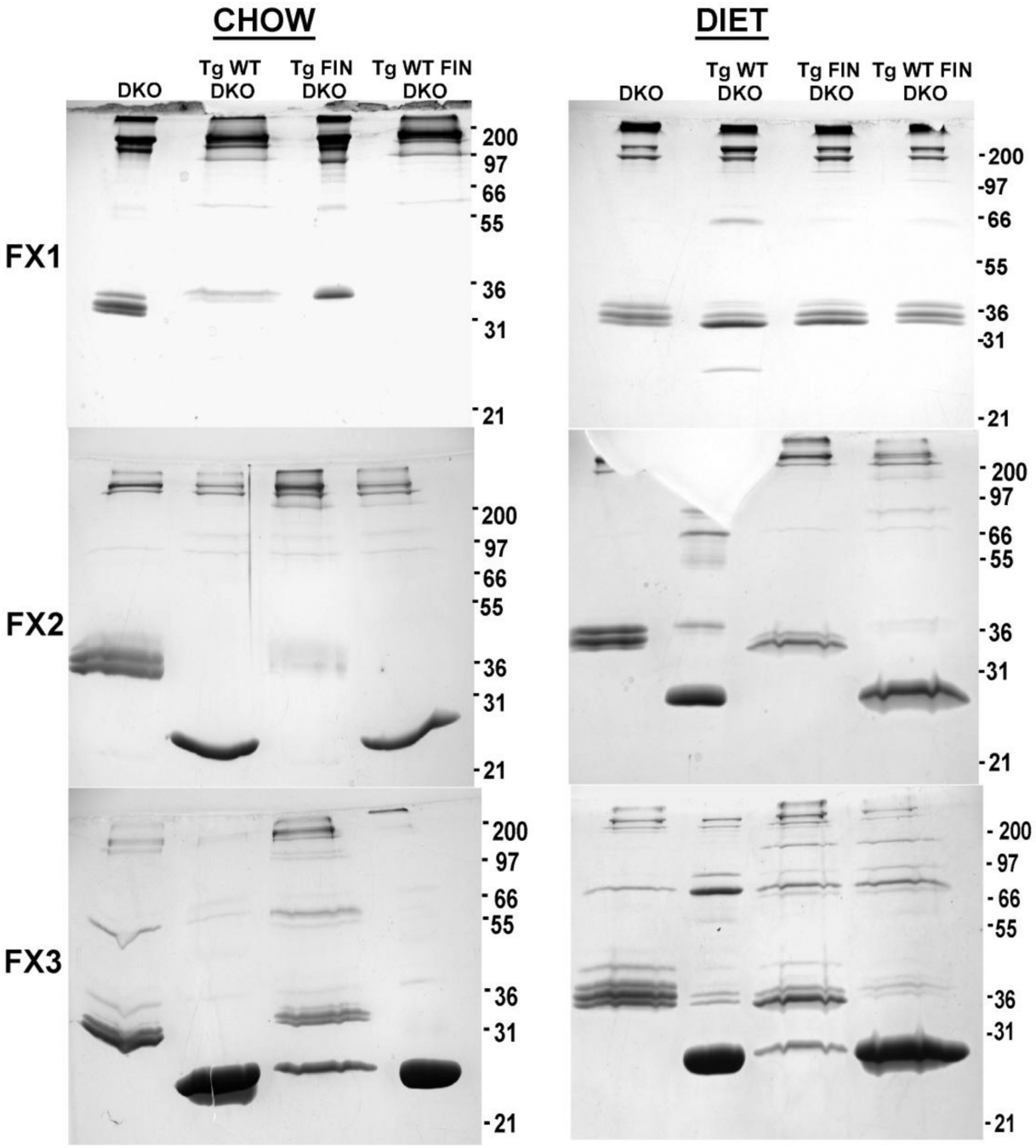


**Figure 4. SDS-PAGE of Lipoprotein Fractions from Chow and Diet-fed Mice**

Panels A and B show SDS-PAGE analysis of plasma FPLC fractions I (VLDL/LDL) II (LDL/HDL) and III (HDL) from chow and atherogenic diet fed mice as separated by FPLC, shown in Figure 1. Each pooled fraction is represented by the equivalent of 10 μg of protein per lane. 12% SDS PAGE gels were run and stained as described in "Materials and Methods". Mouse genotype abbreviations are the same as in Figure 1.

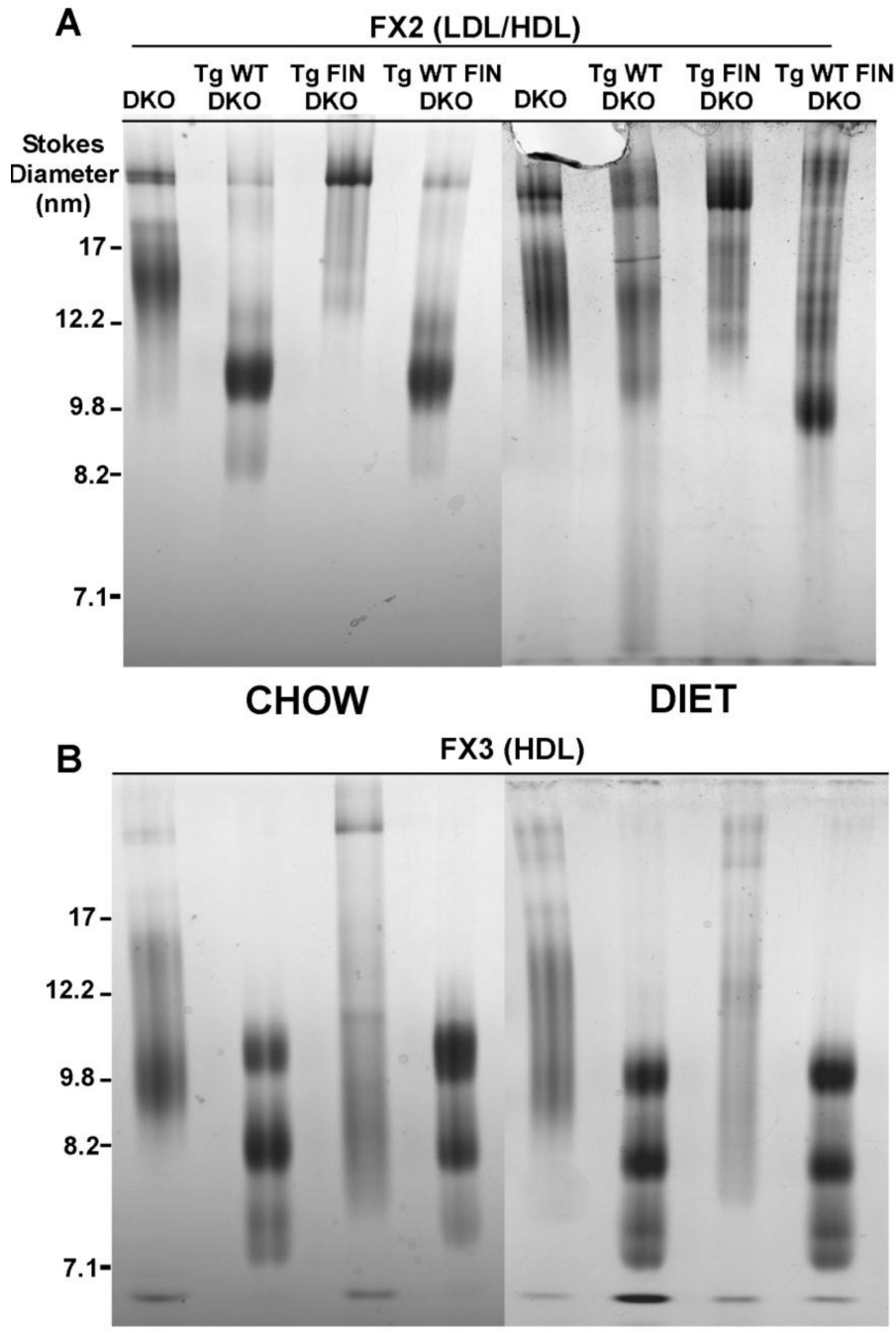


**Figure 5. 4–30% Nondenaturing Gradient Gel Electrophoresis of Lipoprotein Fractions**

Panels A and B show chow- and diet-fed LDL/HDL transition particles and HDL particles isolated from mouse plasma and separated by nondenaturing gradient gel electrophoresis. Gels were loaded with the equivalent of 10 μg of protein per lane, then separated and stained as described in “Materials and Methods” and in the legend to Figure 1. Mouse genotype abbreviations are the same as in Figure 1.

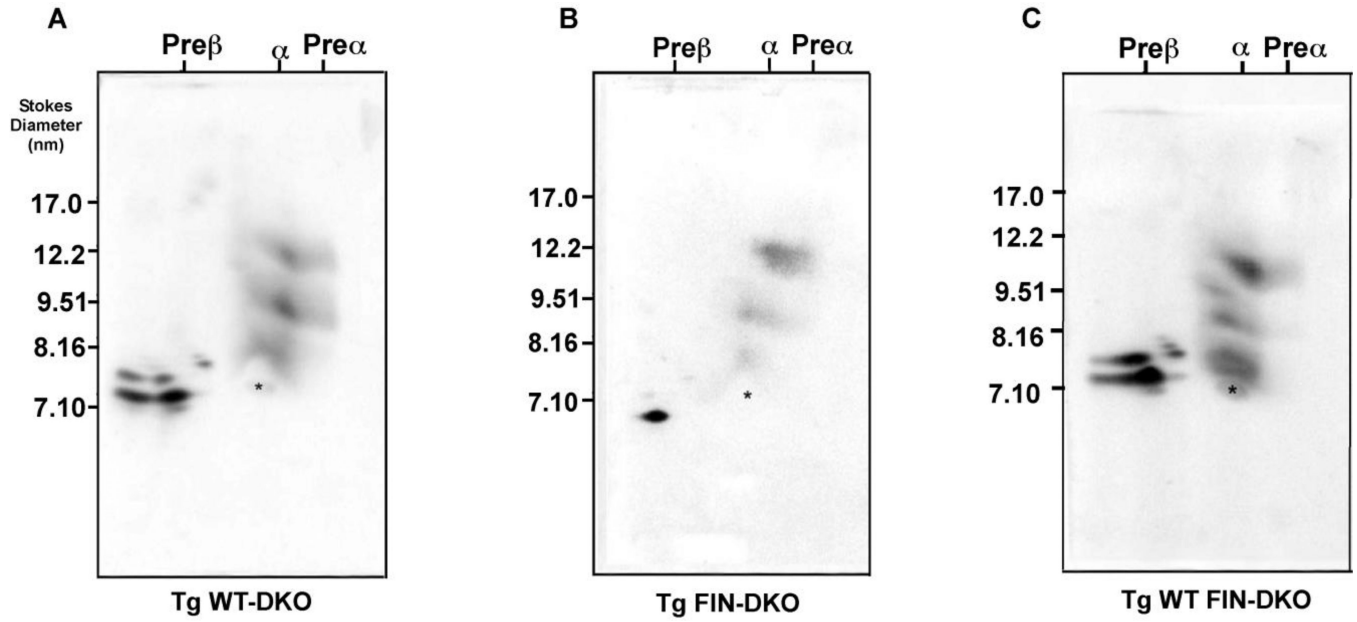


**Figure 6. 2-Dimensional Electrophoresis of HDL from Chow- and Diet- fed Mouse Plasma**

The panels show HDL subclass distribution in plasma of: Panel A shows WT-DKO; Panel B shows FIN-DKO; and Panel C shows, WT FIN-DKO. Total mouse plasma was separated on 2-D gels as described in "Materials and Methods" and in the legend to Figure 1. The asterisk designates the mobility of endogenous serum albumin that marks the α-mobility front. Mouse genotype abbreviations are the same as in Figure 1.

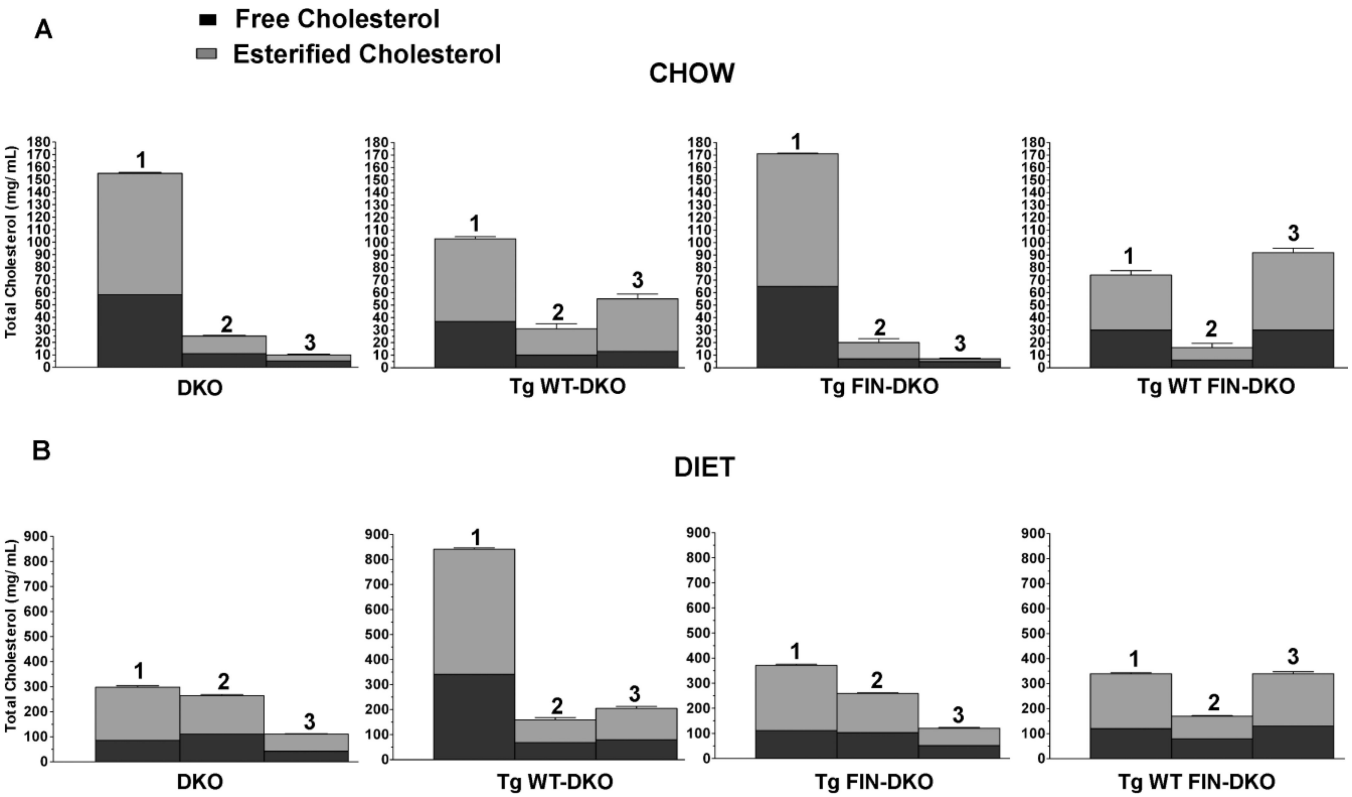


**Figure 7. Free and Esterified Cholesterol Mass in Lipoprotein Fractions**

Panel A shows the free and ester cholesterol values for chow-fed mice and Panel B shows the results for diet-fed mice. Plasma FPLC fractions I (VLDL/LDL), II (LDL/HDL) and III (HDL) were pooled and assayed for free cholesterol and esterified cholesterol as described in “Materials and Methods”. All values represent the mean ± SD for n=4–6 individual experiments. Mouse genotype abbreviations are the same as in Figure 1.

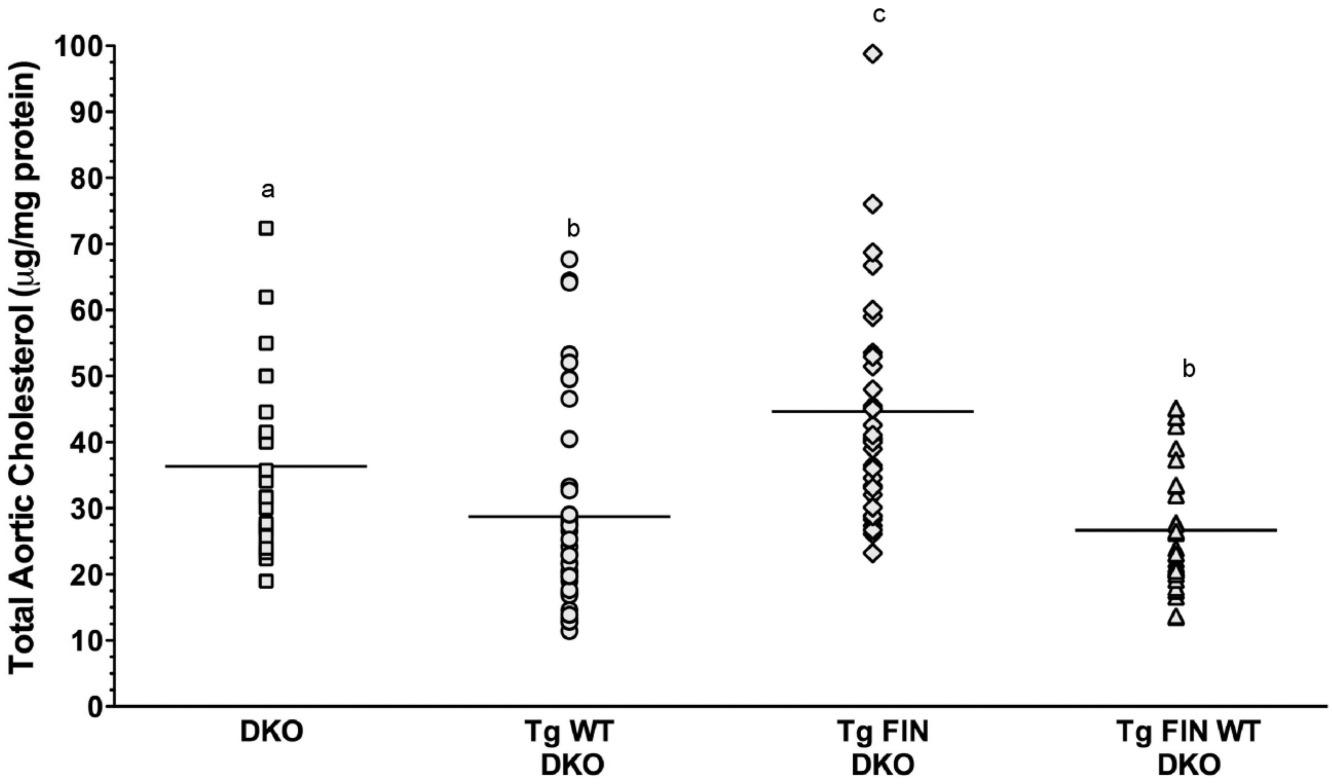


**Figure 8. Atherosclerosis Development In Diet-Fed Transgenic Mice**

Mice were fed an atherogenic diet for 12 wk after which the aortas of DKO, squares; WT-DKO, circles; FIN-DKO, diamonds; and WT FIN-DKO, triangles were analyzed for their cholesterol total content as described in "Materials and Methods". The cholesterol content in each aorta is expressed as μg cholesterol/ mg protein. Male and female mice were averaged together since no statistically significant difference seen among any of the genotypes with respect to gender. The mean of male/ female mice were DKO = 18/17; WT DKO = 10/23; FIN-DKO = 20/19; WT FIN-DKO = 16/18, respectively. Lowercase letters indicate significant difference at $\rho < 0.05$. Mouse genotype abbreviations are the same as in Figure 1.

**Table I**

Plasma Lipid and Apolipoprotein Concentrations in Chow- and Diet-Fed Mice

| Genotype (n) | Plasma Cholesterol (mg/dL) | Plasma Triglycerides (mg/dL) | Human Wild-type ApoA-I (mg/dL) | Human L159R ApoA-I (mg/dL) | Mouse ApoE (mg/dL) |
|---|---|---|---|---|---|
| CHOW | | | | | |
| DKO (10) | 190 ± 19[a] | 126 ± 26[a] | - | - | 7 ± 2[a] |
| WT-DKO (53) | 195 ± 8[a] | 98 ± 8[a] | 100 ± 6[a] | - | 5 ± 1[a] |
| FIN-DKO (37) | 200 ± 13[a] | 120 ± 10[a] | - | 5 ± 1[a] | 17 ± 3[b] |
| WT FIN-DKO (24) | 169 ± 5[a] | 86 ± 5[b] | 113 ± 10[a] | 25 ± 2[b] | 10 ± 2[a,b] |
| DIET | | | | | |
| DKO (24) | 710 ± 19[a] | 226 ± 53[a] | - | - | 22 ± 2[b] |
| WT-DKO (15) | 1201 ± 68[b] | 347 ± 51[a] | 126 ± 16[a] | - | 21 ± 3[b] |
| FIN-DKO (23) | 750 ± 32[a] | 265 ± 14[a] | - | 9 ± 2[a] | 36 ± 2[c] |
| WT FIN-DKO (9) | 850 ± 46[c] | 375 ± 55[a] | 129 ± 19[a] | 38 ± 5[c] | 48 ± 3[c] |

Plasma cholesterol, triglyceride and apolipoprotein values were determined as described in “Materials and Methods.” All values represent the mean ± SD. The number of animals analyzed for each genotype is shown in parenthesis. No statistically significant differences between genders were noted among any of the 4 genotypes. Superscripts with different letters indicate significant differences at $\rho < 0.05$.